ELSEVIER

Chemical Physics 267 (2001) 131–140

Chemical Physics

www.elsevier.nl/locate/chemphys

The influence of molecular structure on strong field energy coupling and partitioning

Alexei N. Markevitch, Noel P. Moore, Robert J. Levis *

Department of Chemistry, Wayne State University, Detroit, MI 48202, USA

Received 4 September 2000

Abstract

Investigating the coupling of polyatomic molecules with intense laser pulses is necessary for understanding strong field photochemistry. Furthermore, the amount of energy deposited in laser/molecule interactions, the degree and pattern of fragmentation, and the energy partitioning between electronic and nuclear motion are of great interest for coherent control experiments in the strong field regime. As a step toward this goal we examine time-of-flight mass and photoelectron spectra for a series of aromatic hydrocarbons – benzene, naphthalene, anthracene and tetracene – collected using 780 nm, 80 fs laser pulses of intensity up to 2×10^{14} W cm^{-2}. For this series, the amount of energy coupled increases with molecular size. The degree of fragmentation increases for the larger molecules, and the kinetic energy distributions of H^+ and C^+ ions and of photoelectrons shift to higher energies. Appearance intensities for ionization and activation of similar fragmentation channels decrease with increasing molecular size. The total amount of energy coupled appears to scale supra linearly with size of these molecules. The measurements suggest that energy deposition into polyatomic molecules occurs by interaction of the laser field with the molecular structure as a whole and not as a result of an interaction of the laser field with a collection of individual atoms. © 2001 Published by Elsevier Science B.V.

1. Introduction

Laser control of quantum dynamics seeks to influence the coupling of radiation into electronic and nuclear modes of molecules by the use of coherent excitation schemes [1,2]. For a growing subset of control applications [3–5], the ability to achieve selective coupling will depend upon understanding of strong field radiation–molecule coupling events. These events are defined by laser intensities producing electric fields on the order of those binding valence electrons to nuclei. When considering the interaction of intense laser pulses and gas phase species, the complexity of the molecular Hamiltonian allows full time-dependent solutions of the Schrödinger equation only for systems of few electrons [6–8]. As this reduces the utility of quantum mechanical approaches for strong field control applications, intrinsically simpler models must be developed if polyatomic molecules are to be considered more fully. Initial semi-classical treatments [9–11] of atoms have been applied to polyatomic molecules. The extensions of atomic models to polyatomic molecules usually approximate the molecule as a sum of couplings of the individual atoms modified by

* Corresponding author. Tel.: +1-313-577-2597; fax: +1-313-577-1377.

E-mail address: levis@chem.wayne.edu (R.J. Levis).

0301-0104/01/$ - see front matter © 2001 Published by Elsevier Science B.V.
PII: S0301-0104(01)00218-X

some factor, such as ratio of molecular/atomic polarizabilities [12] or effective charge on the atoms in consideration [13]. The atom-like models may underestimate the effects of molecular structure on polyatomic molecule/field coupling due to their inability to account for the nature of the molecular electrostatic potential energy surface (PES). The spatial extent of the PES has been included in a *structure-based* field coupling model [14,15]. This model has been used to predict relative tunnel ionization rates for polyatomic molecules [16] and to rationalize an observed evolution in the mechanism of energy coupling in a series of polyatomic molecules [17] and in a single species [18]. We seek in this contribution to elucidate the effect of molecular structure on coupling into both nuclear and electronic degrees of freedom. Here we report that the strong field photoelectron distributions, photofragment distributions and ion kinetic energy distributions shift toward higher energy as the size of a molecule increases. The results imply that molecular structure is important for the coupling mechanism thus suggesting that strong field control of chemical reactivity may be feasible.

The general applicability of various models may be best tested by studying energy coupling trends in a series of similar molecules. The molecules investigated here, benzene (C_6H_6), naphthalene ($C_{10}H_8$), anthracene, ($C_{14}H_{10}$) and tetracene ($C_{18}H_{12}$) are structurally and chemically similar and differ mainly in their molecular size. The term "molecular size" describes both the number of atoms and the spatial extent of these molecules. The spatial extent, defined here as the length of the longest molecular dimension, ranges from 11.7 Bohr in benzene to 24.8 Bohr in tetracene. Under strong-field conditions, benzene, naphthalene and anthracene have been studied previously using photoelectron spectroscopy [17,18] and time-of-flight mass spectrometry [14–16] by this group and other groups [19–22]. The mass spectral measurements revealed limited fragmentation for benzene up to the intensity required to observe the doubly ionized species. Naphthalene revealed more dissociation and anthracene was substantially fragmented at all laser powers. In the present study we focus on the final kinetic energy distributions for fragment ions and photoelectrons to determine the major product channels. Furthermore, mass spectral data for tetracene is now included to test whether any saturation effects in the energy coupling are observed with increasing molecular size. The observed trends in the energy coupling/partitioning are interpreted in terms of the changing molecular structure and highlight the effect of molecular structure on the degree of coupling, the amount of energy coupled into a polyatomic molecule under particular field conditions, and the distribution of energies among all of the possible degrees of freedom.

2. Experimental

To measure ion spectra and ion kinetic energies, a linear 1 m time-of-flight mass spectrometer in dual slope continuous extraction mode was employed. Two complementary measurements of ion kinetic energy release were made. In the first measurement ions were allowed to drift 5 mm in field free conditions prior to being extracted into mass spectrometer. During the drift period ions separate according to their initial velocities. Thus in this experiment a smaller time-of-flight corresponds to a higher initial kinetic energy. In the second experiment, the ion kinetic energy distribution was exposed to a potential barrier before extraction into the time-of-flight system. This allows measurement of the kinetic energy distributions of various ions, as only those ions with sufficient kinetic energy to overcome the known retarding potential are detected. A 1 mm aperture is placed between the ionization and detection regions in order to ensure that only ions generated in the most intense region of the laser beam are collected [23]. The photoelectron spectra were measured using a 30 cm linear time of flight photoelectron spectrometer with *μ-metal* shielded ionization and drift regions. The photoelectron spectrometer had a 500 μm aperture placed between the focal point of the laser beam and the detector.

The excitation source used in these investigations was a 10 Hz regeneratively amplified Ti: sapphire laser similar to one described previously

[14–16], capable of producing pulses of 1.5 mJ, 80 fs centered at 780 nm. The laser intensity was determined by measuring the average pulse energy using a power/energy meter, the unfocussed beam diameter, focal spot size and pulse duration. The calculated and measured focal spot size agreed well with a value of 35 μm. The pulse duration was measured using standard interferometric autocorrelation techniques.

Benzene was introduced effusively into vacuum and solid samples were allowed to sublime directly (the tetracene sample was heated to 90°C to achieve comparable pressure). Spectra were collected with sample pressures of $\approx 2 \times 10^{-6}$ Torr, with background pressures of 2×10^{-8} Torr for both spectrometers.

3. Results

The ion spectra for each of the molecules are presented in Fig. 1 for an intensity of 2×10^{14} W cm^{-2}. For benzene (Fig. 1a), it is observed that the dominant ion is the parent molecular ion, $C_6H_6^+$. Relatively little fragmentation is observed in this molecule. Naphthalene (Fig. 1b) shows diminished parent ion and increased fragmentation in comparison to benzene. Anthracene (Fig. 1c) shows greatly reduced parent ion and extensive fragmentation with lower mass fragments being favored over benzene or naphthalene. The spectrum for tetracene (Fig. 1d) is qualitatively similar to that of anthracene. The occurrence of doubly charged carbon fragments C^{++} also increases with molecular size. The increase of fragmentation with larger molecular size indicates that a greater amount of energy is coupled into the nuclear modes as the molecules become larger. Because the nuclear degrees of freedom scale linearly with the number of atoms, the increasing dissociation as a function of molecular size suggests that the total amount of energy coupled per molecule increases with molecular size.

To further test for the degree of energy coupling as a function of molecular size, the relative kinetic energy releases of the smallest ionic fragments, H^+ and C^+, ejected from these molecules were probed. Fig. 2a and b show time-of-flight distributions of

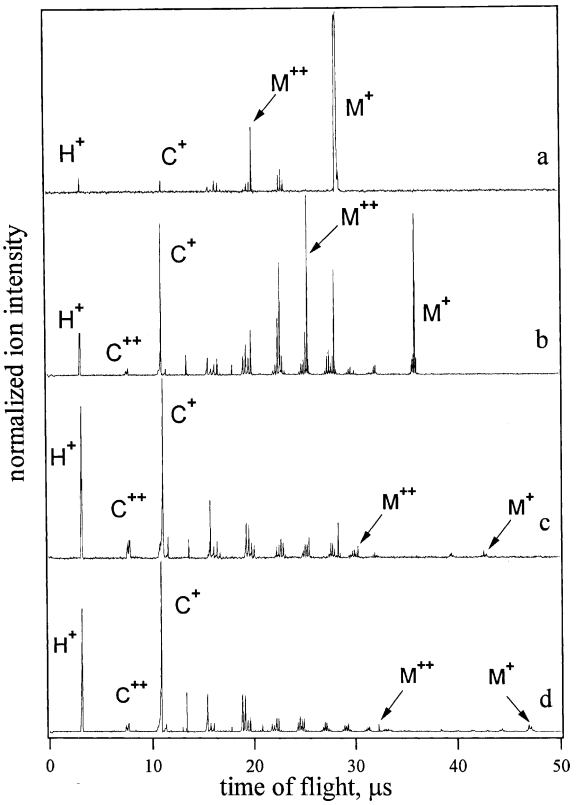

Fig. 1. Time-of-flight mass spectra of (a) benzene, (b) naphthalene, (c) anthracene and, (d) tetracene obtained using 780 nm, 80 fs, 2×10^{14} W cm^{-2} laser pulses.

H^+ and C^+ ions at an intensity of 2×10^{14} W cm^{-2} respectively. In these distributions a smaller time-of-flight corresponds to a larger kinetic energy. The most probable H^+ ion time-of-flight is 3.39 μs for benzene, 3.37 μs for naphthalene, 3.33 μs for anthracene, and 3.29 μs for tetracene. The H^+ cutoff time-of-flight is 3.30 μs for benzene, 3.28 μs for naphthalene, 3.26 μs for anthracene, and 3.19 μs for tetracene. The most probable C^+ ion time-of-flight is 10.7 μs for benzene, 10.7 μs for naphthalene, 10.9 μs for anthracene, and 11.0 μs for tetracene. The C^+ cutoff time-of-flight is 10.1 μs for benzene, 10.3 μs for naphthalene, 10.5 μs for anthracene, and 10.7 μs for tetracene. These trends reveal that the relative kinetic energy releases for H^+ and C^+ increase for the larger molecules in the series. This result is observed for a wide range of laser intensities.

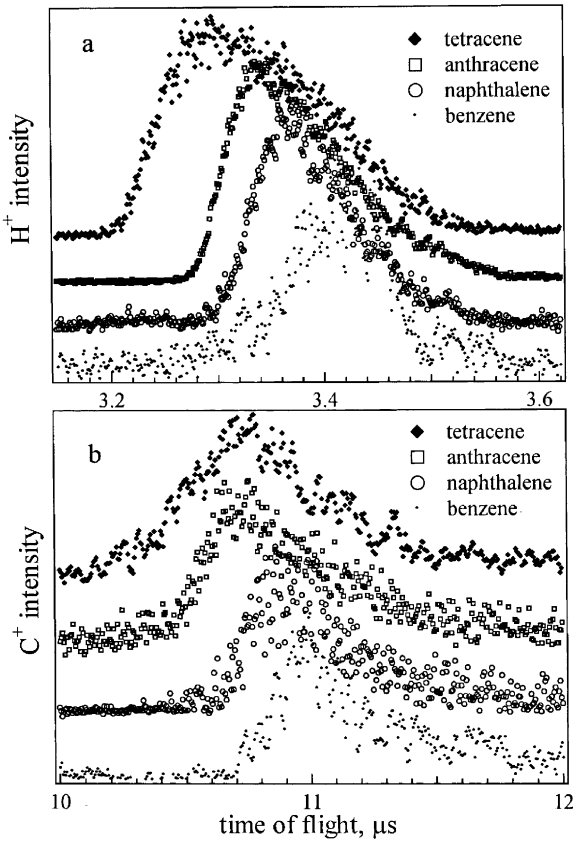

Fig. 2. Zero extraction field measurement of kinetic energy release of (a) H^+ and (b) C^+ eliminated from the molecules using 780 nm, 80 fs, 2×10^{14} W cm^{-2} laser pulses.

To quantify the kinetic energy distributions of the fragments observed in Fig. 2, retarding potential experiments were performed. The relative H^+ ion signals of the four molecules investigated are shown in Fig. 3 as a function of retarding field voltage. Larger retarding voltages are required to minimize the detected ion signal with increasing molecular size at a given laser intensity. This indicates that the energy coupling produces higher energy H^+ ions as the molecular size increases. The maximum kinetic energies of H^+ ions determined in this manner for benzene, naphthalene, anthracene and tetracene are 30, 35, 45, 60 eV respectively. Similar kinetic energies have been obtained in the retarding field measurement of the C^+ ions for all four molecules.

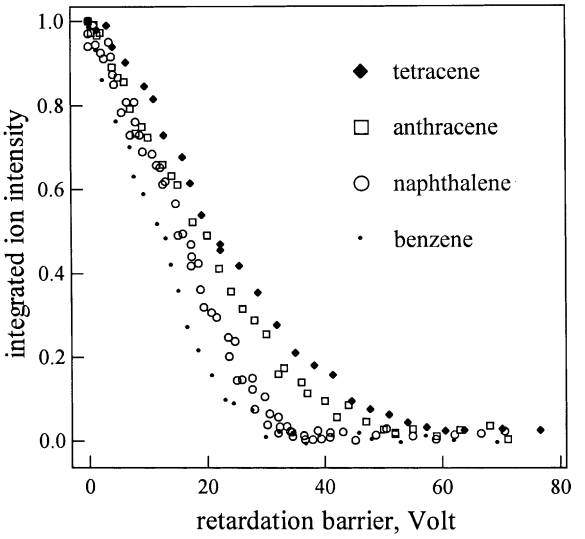

Fig. 3. Retarding field measurement of kinetic energy release of H^+ eliminated from the molecules using 780 nm, 80 fs, 2×10^{14} W cm^{-2} laser pulses.

The fragment kinetic energy distributions from a given species were found to be strongly dependent on the laser intensity employed. Fig. 4 shows the time-of-flight distributions of the H^+ ions liberated from naphthalene, anthracene and tetracene as a function of laser intensity. Each of the molecules was exposed to intensities ranging from 4×10^{12} to 2×10^{14} W cm^{-2}. The appearance intensity for observation of H^+ decreases with increasing molecular size and is 1.2×10^{14} W cm^{-2} for benzene, 8×10^{13} W cm^{-2} for naphthalene, 4×10^{13} W cm^{-2} for anthracene and 2.8×10^{13} W cm^{-2} for tetracene. It is seen that for any given molecule, the time of arrival distributions extend to shorter flight times as the laser intensity is increased. This corresponds to an increase in the mean kinetic energy of a given fragment as the laser intensity increases. In the case of benzene limited H^+ was formed even at the highest intensities.

A plot of the total H^+ ion intensity as a function of laser intensity also reveals the degree of coupling between the laser and the molecules. This measurement reveals both the appearance intensity and relative cross-sections for H^+ production as a function of molecular structure as shown in Fig. 5. The cross-section for production of H^+ from tetra-

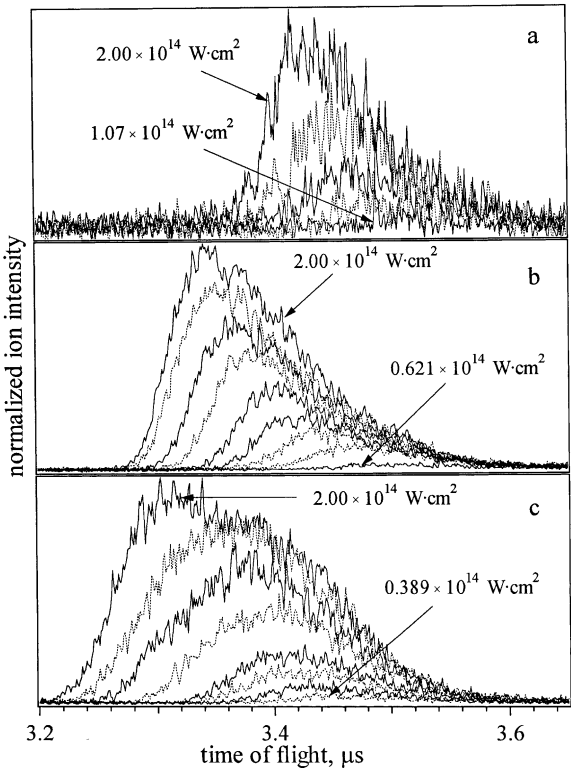

Fig. 4. Zero extraction field measurement of kinetic energy release of H^+ eliminated from of (a) naphthalene at intensities of 2.00, 1.71, 1.46, 1.25 and 1.07×10^{14} W cm^{-2} (b) anthracene at intensities of 2.00, 1.71, 1.46, 1.25, 1.16, 1.07, 0.992, 0.917 and 0.621×10^{14} W cm^{-2} and (c) tetracene at intensities of 2.00, 1.58, 1.25, 0.992, 0.785, 0.621, 0.492 and 0.389×10^{14} W cm^{-2}.

cene is about two orders of magnitude larger than for benzene at the intensity of 1.4×10^{14} W cm^{-2}. We conclude that the production of H^+ from these molecules has strong dependence on molecular structure.

Anisotropy in the direction of the ejected fragment ion can be measured by comparing mass spectra for laser polarization aligned with the time of flight and that for laser polarization rotated by 90°. Pairs of such time-of-flight spectra, taken under zero-field extraction conditions, for naphthalene and anthracene are shown in Fig. 6. It is observed that H^+, C^+, C^{++} and $C_2H_x^+$ fragments are ejected predominantly along the axis of laser polarization. The anisotropy of the direction of ejection of the small ion fragments H^+, C^+, C^{++} and $C_2H_x^+$ is observed for all four molecules.

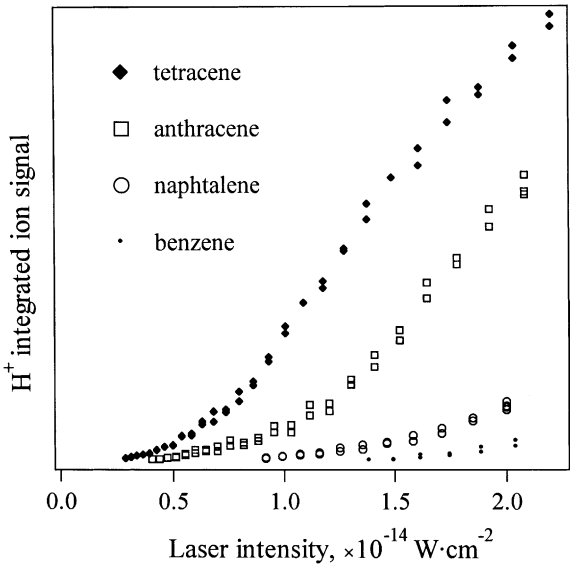

Fig. 5. Integrated ion yield of H^+ eliminated from the molecules as a function of laser intensity.

To probe the quantity of energy coupled into the electronic modes of motion of each molecule we measure the photoelectron kinetic energy distributions. The strong field photoelectron spectra are presented in Fig. 7 for the molecules investigated at an intensity of 1.0×10^{14} W cm^{-2}. The most probable kinetic energy values are 1.7 ± 0.7, 3.0 ± 1.0, 3.2 ± 1.3, and 2.0 ± 0.5 eV for benzene, naphthalene, anthracene and tetracene, respectively. The highest kinetic energy electrons detected for benzene, naphthalene, anthracene and tetracene are 45 ± 5, 80 ± 5, 110 ± 10 and 110 ± 10 eV respectively (the accuracy of the cutoff kinetic energy for anthracene and tetracene is limited by the 2.5 GS/s oscilloscope and the resolution of the photoelectron spectrometer). With the exception of tetracene, it is observed that the maximum kinetic energies recorded increase with molecular size. Again, these measurements suggest that the total amount of energy coupled into these molecules increases with molecular size.

4. Discussion

The data reveal simultaneous increase in energy coupling into both nuclear and electronic modes as

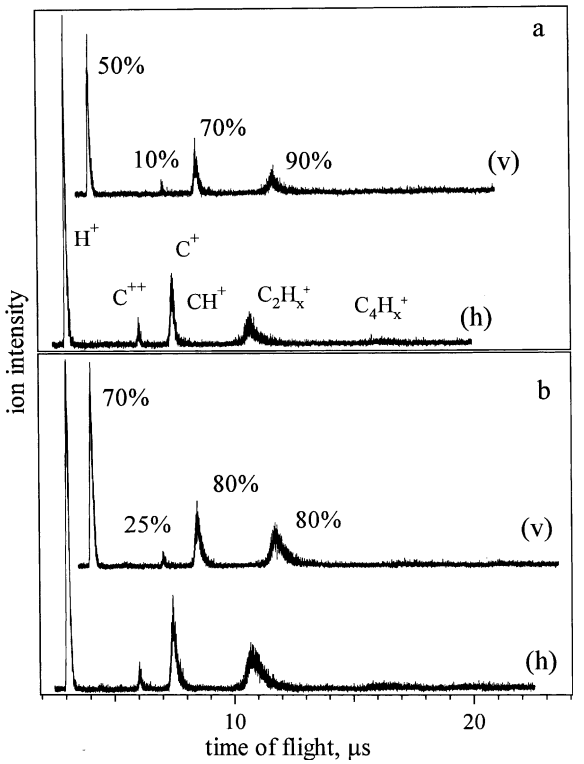

Fig. 6. Time-of-flight spectra for (a) naphthalene and (b) anthracene taken under zero field extraction conditions at the intensity of 1×10^{14} W cm^{-2}, recorded with laser polarized in vertical direction (v) and horizontal direction (h). The horizontal polarization is aligned along the axis of ion extraction. Percentages illustrate the ratio of the areas of the corresponding peaks in each pair of spectra.

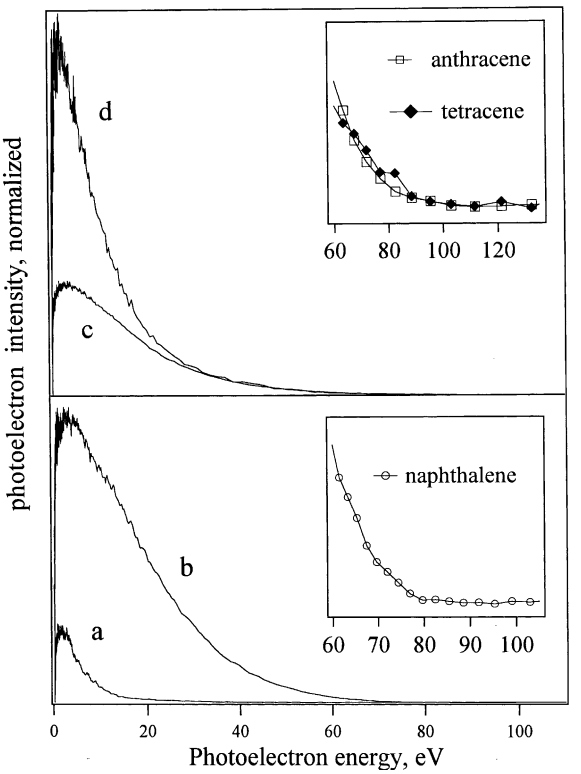

Fig. 7. Photoelectron kinetic energy distribution of (a) benzene (×10), (b) naphthalene (×10), (c) anthracene and, (d) tetracene obtained using 780 nm, 80 fs, 1.0×10^{14} W cm^{-2} laser pulses.

the molecular size increases. These measurements strongly suggest that the total energy deposition increases as molecules become larger in the series. The increasing overall energy deposition in larger molecules is not surprising and could simply be interpreted as a collective effect of an increasing number of atoms interacting with the field independently of each other. However, in such a case the total energy deposition would be expected to scale linearly with molecular size. Thus the energy deposition per atom (and per photoelectron) would be expected to be approximately independent of molecular size. This is clearly not the case, because the degree of fragmentation and of C^{++} production, the photoelectron cutoff energy, and the kinetic energy release of H^+ and C^+ increase for larger molecules. We conclude that the total energy coupled scales supra linearly with size of a molecule in this series.

The appearance intensities for production of ionic fragments (Table 1) and the kinetic energy release of H^+ and C^+ address the question of whether the radiation couples into isolated portions of the molecule, as suggested by the semiclassical treatments [12,13], or into the entire molecule. The appearance intensities and the kinetic energy release of H^+ and C^+ depend strongly on the molecular structure. However, comparison of the properties of the molecules in this series reveals that vibrational frequencies and bond dissociation energies for the C–H and C–C bonds are very similar for these aromatic systems. If energy absorption were localized in such bonds (or individual atoms), the appearance intensities of similar fragmentation channels, the production of the H^+,

Table 1
Measured and calculated properties for the aromatic molecules subjected to strong near-IR field

Molecule	Benzene	Naphthalene	Anthracene	Tetracene
IP (eV)	9.39	8.56	8.05	7.01
Characteristic length (Bohr)	11.7	15.8	20.2	24.8
Molecular ion appearance intensity ($\times 10^{-13}$ W cm^{-2})	4.1	2.6	2.1	1.4
H^+ appearance intensity ($\times 10^{-13}$ W cm^{-2})	11.8	6.96	3.52	2.72
C^+ appearance intensity ($\times 10^{-13}$ W cm^{-2})	14.8	7.24	4.68	3.16
C^{++} appearance intensity ($\times 10^{-13}$ W cm^{-2})	21.4	11.7	7.52	6.72
Calculated relative tunneling probability at 2.5×10^{13} W cm^{-2}	1	30	250	nan (BSI)
Measured relative total ion yield at 5×10^{13} W cm^{-2}	1	10	50	100
Field intensity for onset of BSI ($\times 10^{-13}$ W cm^{-2})	12.2	5.54	3.0	1.50

and the kinetic energy release of H^+ and C^+ would be expected to be relatively independent of the molecular size. As this is clearly opposite of experimental results, we conclude that the energy coupling is not localized in particular bonds (or atoms, or orbitals) and that these molecules do not behave in strong field as collections of atoms absorbing energy independently. To understand the energy deposition into polyatomic molecules, the interaction of laser field with *molecular structure*, should be fully considered. This bonds well for strong field optical control experiments where structure-based contrast mechanism is required.

To understand further the coupling of energy into both nuclear and electronic modes of excitation we employ the structure-based model [14,15]. The model involves the calculation of an electrostatic PES from ab initio methods [24]. Once calculated, the PES is used to obtain the *characteristic length*, a_0, of the molecule, which is defined as the longest distance between classical turning points of the PES at the ionization potential, see Fig. 8. The characteristic length thus obtained is used as the width of a one-dimensional rectangular well with the height given by the ionization potential. This rectangular well has the field strength of the laser superimposed in an attempt to mimic the distortion of the actual PES by the electric field of the laser. The structure-based model allows prediction of the scaling of relative rates of tunnel ionization for a series of molecules by using the WKB transmission coefficient equation [25]:

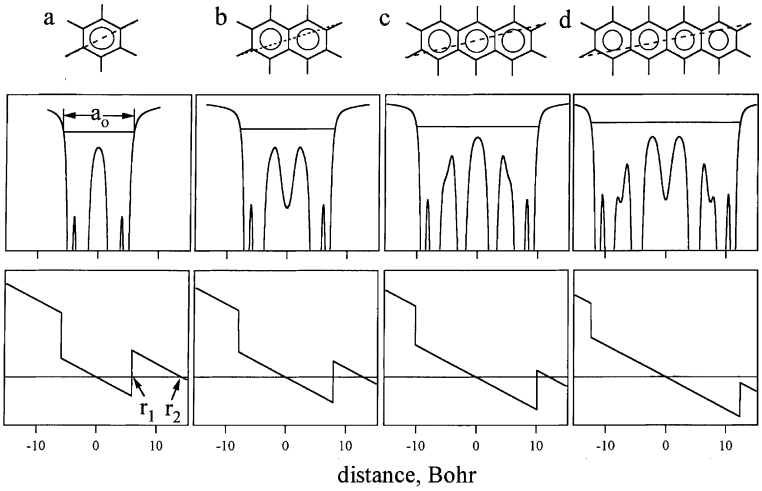

Fig. 8. Molecular structures, electrostatic PESs, and rectangular wells approximating the extent of PES with 1.25 V/Å electric field superimposed for (a) benzene, (b) naphthalene, (c) anthracene and, (d) tetracene. The dotted line in the top panel displays the vector employed for the characteristic length.

$$T = \exp\left\{ -2\int_{r_1}^{r_2} 2[V(r) - E]^{1/2} \mathrm{d}r \right\} \quad (1)$$

where $V(r)$ is the functional form of the barrier to tunnel ionization, E is the ground state energy of an electron inside the perturbed PES, and r_1 and r_2 are the classical turning points of the barrier, see Fig. 8. According to the structure-based model, as the characteristic length increases, the potential barrier to tunneling is reduced relative to the electron ground state energy. Fig. 8 shows the molecular structure and one-dimensional PESs associated with each molecule in this series. The rectangular wells generated using the structure-based model each have an electric field of 1.25 V/Å superimposed across their widths. According to the model, the barrier to tunneling ionization is significant for benzene, decreases for naphthalene and anthracene, and disappears for tetracene. This model suggests that the degree of laser/molecule coupling increases with molecular size at the same field intensity. A similar degree of laser/molecule coupling (activation of similar energy coupling channels) is expected at lower field intensities as molecular size increases in this series.

The structure-based model can be used to calculate the relative rates of tunnel ionization, to predict field intensity for onset of barrier suppression ionization (BSI), and also to determine whether tunnel ionization is expected to play a significant role (vs. MPI) at a particular field intensity. Some calculated and experimental values are presented in Table 1. Both the experimental data and the calculations using the structure-based model reveal that lower field intensities are required to activate similar processes (similar energy coupling channels) as the molecular size increases.

Although the structure-based model qualitatively predicts the increased degree of energy deposition with increasing characteristic length, it does not make any predictions regarding the coupling of the laser field into either electronic or nuclear degrees of freedom. The structure-based model is a static model, but these molecules are subjected to an alternating electric field. This field induces an oscillatory motion of polarized electrons (primarily valence electrons) inside the PES. In a weak field non-resonant case, only the linear polarization is induced, and the interaction is mostly elastic, predominantly scattering rather than absorbing radiation. As the field becomes stronger, higher order non-linear susceptibilities start to play role in the optical response and the field/molecule interaction becomes increasingly inelastic. An increase in characteristic length results in a greater freedom for the electrons to move in response to the driving electric field and, consequently, in higher dynamic polarizabilities [26]. This higher dynamic polarizability is synonymous with a higher mobility of charges driven by the electric field [26]. The data shown here is consistent with the hypothesis that at a given field intensity, a longer characteristic length facilitates acceleration of the electrons inside the PES to higher kinetic energies. As the molecular size increases some saturation of energy coupling trends is expected and the data presented here are in keeping with that premise. Note that the photoelecton spectra, the degree of fragmentation and the amount C^{++} produced from anthracene and tetracene are similar and may indicate the onset of saturation of energy coupling into these channels. On the other hand, the data on the kinetic energy release of H^+ and C^+ eliminated from these molecules show no saturation effects.

On the time scale of the laser pulse the electric field couples predominantly into electronic modes of excitation. The measured fragmentation patterns result from nuclear motion subsequent to, and presumably resulting from the electronic excitation. A significant amount of Coulomb repulsion is necessary to explain the ion kinetic energies up to 60 eV observed in his experiment. Note that these kinetic energies suggest that a gentle dissociation of C–C and C–H bonds is not occurring. Coupling of the laser field into the nuclear coordinates during the 80 fs laser pulse is expected to result only in a moderate increase in the fragment ion kinetic energies. The coupling mechanism operating here must be different from a Coulomb explosion observed of small molecules. For example, the kinetic energy releases observed in this experiment depend strongly on the laser pulse intensity while they do not in the case of diatomic Coulomb explosion [27–29]. It is possible that the coupling mechanism operating here is similar to

the mechanisms considered in strong field Coulomb explosion of C_{60} [30] and Coulomb explosion of molecular clusters [31,32].

Finally, we consider how orientation averaging [33] may affect the scaling of experimental values in comparison with calculations in which only the longest coupling length for each molecule is employed. We should note here, that no evidence supporting orientation averaging was found in recent experiments on strong field ionization of smaller sized molecules [19]. Nevertheless, because the ion fragments are ejected predominantly along the direction of laser polarization, we believe that coupling is sensitive to the relative alignment of a molecule with polarization of the laser in this experiment. The orientation averaging should play an important role in interpretation of the data as it may mask the trend of increased energy coupling with increasing molecular size. As large molecules are not aligned at these intensities by 80 fs laser pulses [34,35], the laser field couples in these molecules through all possible distribution of coupling lengths. While a highly symmetric molecule, such as benzene (D_6h), has a relatively small range of coupling lengths, an elongated molecule, like tetracene (D_2h), has an increased range of coupling lengths. Fields couple into tetracene through orientations similar to benzene, plus many others. One of the effects of orientation averaging may be the simultaneous presence of cold fragmentation channels resulting in the production of M^+ and large ion fragments and hot fragmentation channels resulting in the production of H^+, C^+ and C^{++} in the ion spectra of larger molecules in the series. The wide distribution of lengths may decrease the most probable photoelectron kinetic in comparison to those that might be observed if molecules were coupled through characteristic length only. In spite of the possible masking by orientation averaging the trend of increasing coupling of the field into fragmentation channels with increasing molecular size is still apparent.

5. Conclusion

In conclusion, we have presented strong field ion and photoelectron spectroscopy of a series of similar molecules with increasing size. We observe that as the molecular size increases, more energy is coupled into photoelectron kinetic energy and fragmentation channels. From the measured energy coupling trends, it appears that the total amount of energy coupled during such interaction scales faster than linearly with molecular size in this series. The trend of increased coupling with increasing molecular size is predicted by the structure-based coupling model which takes into account the extent of perturbation of electrostatic molecular PES by the electric field of the laser. This work presents an insight into energy coupling and partitioning in the strong field ionization and fragmentation of polyatomic molecules. It demonstrates that polyatomic molecules do not couple with the field as a collection of individually absorbing atoms. The interaction of polyatomic molecules with the laser field is shown to depend strongly on molecular structure. As the viability and success of a certain subset of control experiments depend on the ability to independently influence coupling channels, experiments of this nature may provide an underlying framework of useful knowledge.

Acknowledgements

This work has been supported by the National Science Foundation Young Investigator Award (RJL) and CHE-9976476. We also acknowledge the generous support of the Dreyfus and Sloan Foundations. RJL is a Camille Dreyfus Teacher-Scholar and a Sloan fellow.

References

[1] A. Peirce, M. Dahleh, H. Rabitz, Phys. Rev. A 37 (1988) 4950.
[2] H. Rabitz, R. de Vivie-Riedle, M. Motzkus, K. Kompa, Science 288 (2000) 824.
[3] C.J. Bardeen, J.W. Che, K.R. Wilson, V.V. Yakovlev, P.J. Kong, B. Kohler, J.L. Krause, M. Messina, J. Chem. Phys. 101 (1997) 3815.
[4] T.C. Weinacht, J.L. White, P.H. Bucksbaum, J. Phys. Chem. A 103 (1999) 10166.

[5] A. Assion, T. Baumert, M. Bergt, T. Brixner, B. Kiefer, V. Seyfried, M. Strehle, G. Gerber, Science 282 (1998) 824.
[6] S. Chelkowski, C. Foisy, A.D. Bandrauk, Phys. Rev. A 57 (1998) 1176.
[7] H. Yu, T. Zuo, A.D. Bandrauk, J. Phys. B: At. Mol. Opt. 31 (1998) 1533.
[8] H. Yu, A.D. Bandrauk, Phys. Rev. A 56 (1997) 685.
[9] L.V. Keldysh, Zh. Eksp. Teor. Fiz. 47 (1964) 1945 [Sov. Phys. JETP 20 (1965) 1307].
[10] A.M. Perelomov, V.S. Popov, M.V. Terent'ev, Sov. Phys. JETP 23 (1966) 924.
[11] M.V. Ammosov, N.B. Delone, V.P. Krainov, Zh. Eksp. Teor. Fiz. 91 (1986) 2008 [Sov. Phys. JETP 64 (1986) 1191].
[12] S.L. Chin, P. Golovinski, J. Phys. B: At. Mol. Opt. Phys. 30 (1997) 2403.
[13] A. Tabelepour, S. Larochelle, S.L. Chin, J. Phys. B: At. Mol. Opt. Phys. 31 (1998) 2769.
[14] M.J. DeWitt, R.J. Levis, J. Chem. Phys. 110 (1999) 11368.
[15] R.J. Levis, M.J. DeWitt, J. Phys. Chem. 103 (1999) 6493.
[16] M.J. DeWitt, R.J. Levis, J. Chem. Phys. 108 (1998) 7739.
[17] M.J. DeWitt, R.J. Levis, Phys. Rev. Lett. 81 (1998) 5101.
[18] N.P. Moore, R.J. Levis, J. Chem. Phys., submitted for publication.
[19] S.M. Hankin, D.M. Villeneuve, P.B. Corkum, D.M. Rayner, Phys. Rev. Lett. 84 (2000) 5082.
[20] M. Castillejo, S. Couris, E. Koudoumas, M. Martín, Chem. Phys. Lett. 308 (1999) 373.
[21] K.W.D. Ledingham, R.P. Singhal, D.J. Smith, T. McCanny, P. Graham, H.S. Kilic, W.X. Peng, S.L. Wang, A.J. Langley, P.F. Taday, C. Kosmidis, J. Phys. Chem. A 102 (1998) 3002.
[22] K.W.D. Ledingham, R.P. Singhal, D.J. Smith, T. McCanny, P. Graham, H.S. Kilic, W.X. Peng, A.J. Langley, P.F. Taday, C. Kosmidis, J. Phys. Chem. A 103 (1999) 2952.
[23] M.A. Walker, P. Hansch, L.D. Van Woerkom, Phys. Rev. A 57 (1998) R701.
[24] GAUSSIAN 99, Development Version (Revision B.08) M.J. Frisch, G.W. Trucks, H.B. Schlegel, G.E. Scuseria, M.A. Robb, J.R. Cheeseman, V.G. Zakrzewski, J.A. Montgomery Jr., R.E. Stratmann, J.C. Burant, S. Dapprich, J.M. Millam, A.D. Daniels, K.N. Kudin, M.C. Strain, O. Farkas, J. Tomasi, V. Barone, B. Mennucci, M. Cossi, C. Adamo, J. Jaramillo, R. Cammi, C. Pomelli, J. Ochterski, G.A. Petersson, P.Y. Ayala, K. Morokuma, D.K. Malick, A.D. Rabuck, K. Raghavachari, J.B. Foresman, J.V. Ortiz, Q. Cui, A.G. Baboul, S. Clifford, J. Cioslowski, B.B. Stefanov, G. Liu, A. Liashenko, P. Piskorz, I. Komaromi, R. Gomperts, R.L. Martin, D.J. Fox, T. Keith, M.A. Al-Laham, C.Y. Peng, A. Nanayakkara, M. Challacombe, P.M.W. Gill, B. Johnson, W. Chen, M.W. Wong, J.L. Andres, C. Gonzalez, M. Head-Gordon, E.S. Replogle, J.A. Pople, Gaussian Inc., Pittsburgh, PA, 2000.
[25] D. Bohm, Quantum Theory, Prentice-Hall, New York, 1951.
[26] M. Schulz, S. Tretiak, V. Chernyak, S. Mukamel, J. Am. Chem. Soc. 122 (2000) 452.
[27] T. Seideman, M.Yu. Ivanov, P.B. Corkum, Phys. Rev. Lett. 75 (1995) 2819.
[28] C. Cornaggia, M. Schmidt, D. Normand, Phys. Rev. A 51 (1995) 1431.
[29] L.J. Frasinski, K. Codling, P. Hatherly, J. Barr, I.N. Ross, W.T. Toner, Phys. Rev. Lett. 58 (1987) 2424.
[30] R.C. Contantinescu, S. Hunsche, H.B. Van Linden van den Heuvell, H.G. Muller, Phys. Rev. A 58 (1998) 4637.
[31] J.V. Ford, Q. Zhong, L. Poth, A.W. Casteleman Jr., J. Chem. Phys. 110 (1999) 6257.
[32] J.V. Ford, Q. Zhong, L. Poth, A.W. Casteleman Jr., Int. J. Mass Spectrom. 192 (1999) 327.
[33] M.J. DeWitt, B.S. Prall, R.J. Levis, J. Chem. Phys. 113 (2000) 1553.
[34] J.S. Posthumus, J. Plumridge, M.K. Thomas, K. Codling, L.J. Frasinki, A.J. Langley, P.F. Taday, J. Phys. B: At. Mol. Opt. Phys. 31 (1998) L553.
[35] J.S. Posthumus, J. Plumridge, L.J. Frasinki, K. Codling, A.J. Langley, P.F. Taday, J. Phys. B: At. Mol. Opt. Phys. 31 (1998) L985.